Available online at www.sciencedirect.com

SciVerse ScienceDirect

Ceramics International 39 (2013) 4937–4944

CERAMICS INTERNATIONAL

www.elsevier.com/locate/ceramint

Antibacterial ciprofloxacin HCl incorporated polyurethane composite nanofibers via electrospinning for biomedical applications

Yuri Choi[a], R. Nirmala[a,*], Jun Yeoub Lee[a], Mashiar Rahman[b], Seong-Tshool Hong[b], Hak Yong Kim[a,*]

[a]*Department of Organic Materials and Fiber Engineering, Chonbuk National University, Jeonju 561-756, South Korea*
[b]*Department of Microbiology and Genetics , Institute for Medical Science, Chonbuk National University, Jeonju 561-756, South Korea*

Received 14 November 2012; received in revised form 26 November 2012; accepted 26 November 2012
Available online 8 December 2012

Abstract

We report on the preparation and characterization of polyurethane (PU) composite nanofibers by electrospinning. Two different approaches were adopted to obtain the PU composite nanofibers. In the first approach, a homogeneous solution of 10 wt% PU containing ciprofloxacin HCl (CipHCl) drug was electrospun to obtain PU/Drug composite nanofibers. And in the second approach, the PU with ciprofloxacin HCl drug and ceramic hydroxyapatite (HA) particles were electrospun to obtain the PU/Drug and PU/Drug/HA composite nanofibers. The surface morphology, structure, bonding configuration, optical and thermal properties of the resultant products were characterized by scanning electron microscopy (SEM), X-ray diffraction (XRD), Fourier transform infrared spectroscopy (FT-IR), differential scanning calorimetry (DSC), thermogravimetric analysis (TGA) and UV–vis spectroscopy. The antibacterial activity was tested against common food borne pathogenic bacteria, namely, *Staphylococcus aureus*, *Escherichia coli* by the minimum inhibitory concentration (MIC) method. Our result results demonstrate that these composite nanofibers possess superior characteristics which can utilized for variety of applications.

Keywords: Antibacterial activity; Composite nanofibers; Eletrospinning; Polyurethane

1. Introduction

Polyurethane (PU) polymer has a broad spectrum of commercial applications in many market areas because of their excellent chemical and physical properties [1]. These polymers are synthesized from poly addition reactions of isocyanate and hydroxyl groups [2]. PU dispersions have found diverse applications in different industries like textile, adhesives, gloves, wood finishing, glass fiber sizing, automotive top coating films for packaging and other applications [3]. PU is frequently used in wound dressings because of its good barrier properties and oxygen permeability. PU foam and elastomer have been used as cushion insole material in footwear [4]. Recently, the design and synthesis of new polymer/nanosized inorganic composite materials have been widely investigated in order to combine the properties of inorganic fillers and polymer matrices which can be utilized for many technological applications [5–9]. In this connection, wound dressing from electrospun nanofibers potentially offers many advantages over conventional processes [10]. Immediate care of skin wounds is important for prevention of microbial infection and trans-epidermal water loss leading to acceleration of wound regeneration [11]. Electrospinning has attracted much attention as a simple and versatile technique capable of generating continuous nanofibers with novel properties including high surface-to-volume ratio, good mechanical properties and high aspect ratio [12,13]. Generally, the ultimate goal of the nanofiber design is to provide an ideal structure that can replace the natural extra cellular matrix until the host cells can grow and synthesize a new natural cellular matrix [6].

Extensive studies have been conducted to develop biocompatible electrospun nanofibrous scaffolds for wound dressing

*Corresponding authors. Tel.: +82 63 270 2351; fax: +82 63 270 4249.
E-mail addresses: nim_jbnu@yahoo.com (R. Nirmala), khy@jbnu.ac.kr (H.Y. Kim).

0272-8842/$ - see front matter © 2012 Elsevier Ltd and Techna Group S.r.l. All rights reserved.
http://dx.doi.org/10.1016/j.ceramint.2012.11.088

applications. An electrospun nanofiber membrane containing antibiotic agents has been used as a barrier to prevent the post-wound infections. The combination of both of these properties can result in a perfect wound dressing material. Among them, ciprofloxacin HCl (CipHCl), a fluoroquinolone antibiotic, is one of the most widely used antibiotics for wound healing because of its low minimal inhibitory concentration for both Gram-positive and Gram-negative bacteria that cause wound infections [14] and the frequency of spontaneous resistance to ciprofloxacin is very low [15]. On the other hand, hydroxyapatite (HA) is chemically similar to the inorganic component of bone matrix—a very complex tissue with general formula $Ca_{10}(OH)_2(PO_4)_6$. The close chemical similarity of HA to natural bone has led to extensive research efforts to use synthetic HA as a bone substitute and/or replacement in biomedical applications [16,17]. Recently, HA has been used for a variety of biomedical applications, including matrices for drug release control and bone tissue engineering materials [18,19]. HA exhibits excellent biocompatibility with soft tissues such as skin, muscle and gums. Such capabilities have made HA an ideal candidate for orthopedic and dental implants or components of implants [20]. HA nano-and microcrystals with multiform morphologies (separated nanowires, nanorods, microspheres, microflowers and microsheets) have been successfully synthesized by many powder processing techniques, including sol–gel synthesis [21–25], solid state reactions [26], co-precipitation [27], hydrothermal reactions [28], micro-emulsion syntheses [29] and mechanochemical synthesis [30]. So in this work, we utilize both cipHCl and HA to prepare the composite nanofibrous wound dressing material via the electrospinning technique. Blending of Drug and Drug/HA into PU nanofibers has attracted a great deal of attention in biomedical applications because the resulting nanofibers have very strong antimicrobial activity. The resultant composite materials can be utilized for many technological applications such as wound dressing, food packaging and other biomedical uses. This study involves the characterization of these nanofibers and biocompatibility of these scaffolds along with the simultaneous antibacterial activity of CipHCl. Such kinds of materials can have much improved properties in terms of thermal stability, flexibility and solubility with that of the pristine PU. Additionally, to our best of knowledge, there have been no reports based on these composite nanofibers.

In this study, we prepared pristine PU nanofibers, PU/Drug and PU/Drug/HA composite nanofibers by using electrospinning process. The resultant composite nanofibers PU, PU/Drug and PU/Drug/HA were characterized by scanning electron microscopy (SEM), energy dispersive X-ray analysis (EDX), X-ray diffraction (XRD), Fourier transform (FT-IR), differential scanning calorimeter (DSC), thermogravimetric analysis (TGA) and UV–vis spectroscopy. The antibacterial activity of the PU composite nanofibers were tested against common food borne pathogenic bacteria namely, *Staphylococcus aureus*, *Escherichia coli*, by the minimum inhibitory concentration (MIC) method.

2. Experimental

2.1. Materials

Polyurethane (PU, MW = 110,000) purchased from Cardio Tech, CipHCl (drug) was supplied from LKT laboratories, Inc., USA. Tetrahydro furan (THF) and N,N-dimethylformamide (DMF) (analytical grade, Showa, Japan) were used as solvents without further purification. Biomimetic hydroxyapatite is gifted by Professor Hak Yong Kim and the detailed synthesis procedure has been reported in [31] and the references therein. *S. aureus* (KCCM 29231), *E. coli* (KCCM 52922), were purchased from Korean Culture Center of Microorganisms (KCCM). These pathogenic microorganisms were used as the model bacteria for the disc diffusion susceptibility test. For the bactericidal activity measurement Mueller-Hinton broth (MHB) & Mueller-Hinton agar (MHA) (Difco, Sparks, MD, USA) were used.

2.2. Electrospinning

Two different approaches were adopted to incorporate the drug and the HA particles in to PU nanofibers. In the first method, PU solution with 10 wt% was prepared by dissolving in THF and DMF with the ratio of 1:1. HA 2%: Drug 1.5% solution was prepared and then added to the PU with 10 wt% of the polymer solution. The final homogenous mixture was used to electrospinning. Herein, the resultant composite nanofibers are named as PU, PU/Drug and PU/Drug/HA. A high voltage power supply (CPS-60 K02V1, Chungpa EMT, South Korea) of 15 kV to the syringe micro-tip was supplied to electrospin the nanofibers, whereas a ground iron drum covered by blue paper served as counter electrode. In our study, we used the conventional electrospinning setup, where the syringe has been kept inclined to flow the spinning solution. The tip-to-collector distance was kept at 15 cm. Polymer solution was fed to the 5 mL syringe with plastic micro-tip. All the experiments were conducted at room temperature. These experimental parameters were chosen from an optimization of a series experiments. The developed nanofiber mats formed were collected on the rotating drum covered with the collecting blue paper.

2.3. Characterizations

The morphology of the PU, PU/Drug and PU/Drug/HA composite nanofibers was observed by using scanning electron microscopy (SEM, Hitachi S-7400, Hitachi, Japan). Elemental composition analyses of the thin films were carried out by using a SEM equipped with an energy dispersive X-ray (EDX) spectrometer. Structural characterization was carried out by X-ray diffraction (XRD) in a Rigaku X-ray diffractometer operated with Cu Kα radiation ($\lambda = 1.540$ Å), The bonding configurations of the samples were characterized by means of Fourier transform

infrared (FT-IR). Differential scanning calorimetry (DSC, Perkin–Elmer, USA) characterizations were performed for the PU composite nanofibers under nitrogen ambient with a flow rate of 20 mL/min. The samples were heated from room temperature to 200 °C at a scanning rate of 10 °C/min. Thermogravimetric analysis (TGA, Perkin–Elmer, USA) was carried out for the composite nanofibers under nitrogen ambient with a flow rate of 20 mL/min. The samples were heated from 30 to 800 °C at a rate of 10 °C/min). The UV–vis spectra were measured in the range of 200–800 nm by using a UV–vis spectrometer (Lambda 900, Perkin–Elmer, USA).

2.4. Bactericidal activity by the disc diffusion susceptibility test

The disc diffusion susceptibility test for *S. aureus*, *E. coli*, was performed on the MHA plate at the incubation temperature of 37 °C. The MHB containing 1.5×10^6 colony-forming units (cfu) of bacteria were used for the lawn culture. The PU, PU/Drug and PU/Drug/HA composite nanofibers were cut into 6 mm diameter discs. Then, each bacterium was lawn cultured on the MHA Petri plate by using a sterile cotton swab. The ultraviolet sterilized PU containing Drug and Drug/HA composite nanofibers discs were kept at uniform distance and then incubated overnight at 37 °C. The zone of inhibition was observed after 24 h of incubation and the diameter of the zone was measured.

3. Results and Discussion

Fig. 1(a)–(c) shows the SEM images of the as-obtained pristine PU, PU/Drug and PU/Drug/HA composite nanofibers. As shown in these figures, the pristine and composite nanofibers were observed to be smooth and bead-free nanofibers. Fig. 1(a) shows the electrospun nanofibers from pure PU solution. It is clearly seen as shown in this image that smooth, bead-free, and continuous nanofibers are formed by pristine PU. However, the morphological appearance of the PU/Drug, PU/Drug/HA composite nanofibers synthesized was slightly differed from each other as shown in Fig. 1(b) and (c). The electrospun PU/Drug composite nanofibers obtained from the homogenous solution showed that the incorporation of the drug into the nanofibers not only dramatically decreased their average diameter but also reduced the diameter distribution of electrospun nanofibers. The diameter of the nanofibers is in the range of 200–250 nm. However, in the case of the PU/Drug/HA composite nanofibers appear to be protruded outwards at the periphery of the nanofibers. The diameter of the nanofibers is in the range of 150–200 nm. It is significantly noted that the diameter of the pristine PU nanofibers was slightly larger than that of the PU/Drug and PU/Drug/HA composite nanofibers which is attributed to the partial agglomerization of blended nanoparticles during the electrospinning process. The composite electrospun

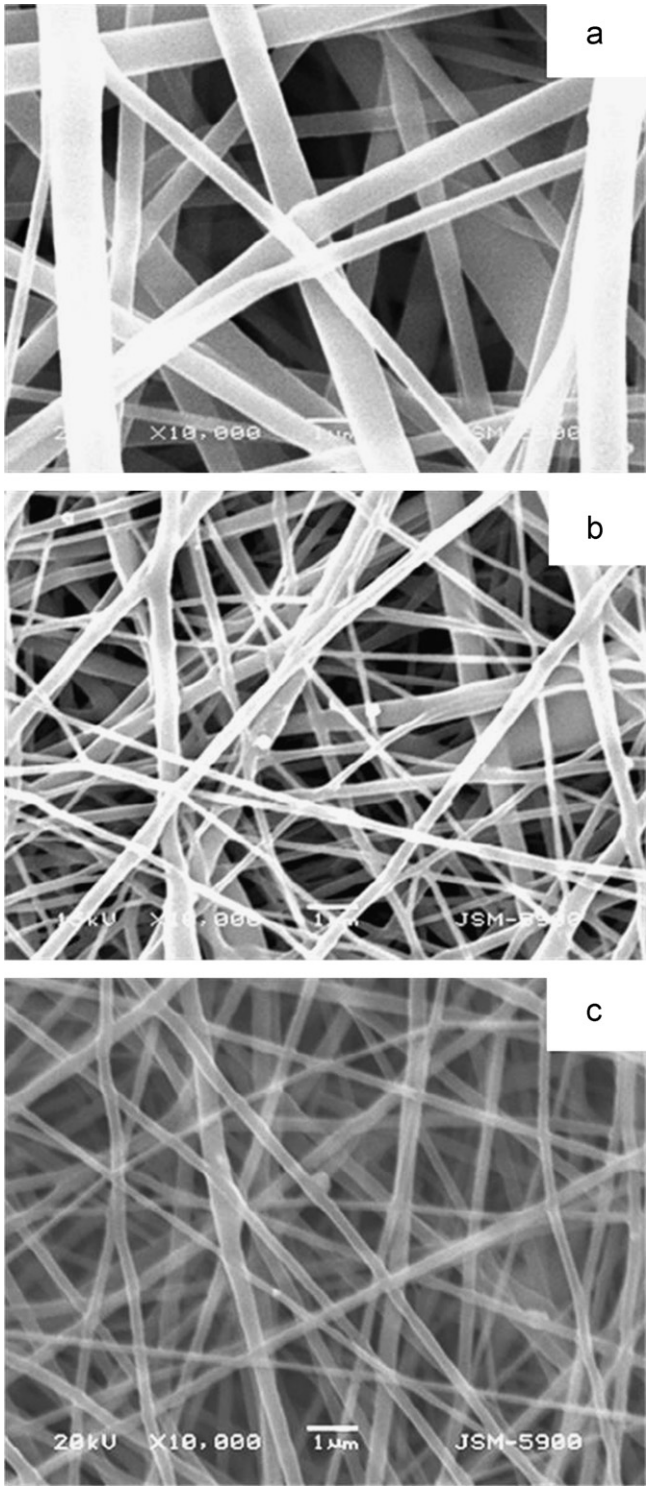

Fig. 1. SEM images of (a) PU, (b) PU/Drug and (c) PU/Drug/HA nanofibers.

nanofiber mat produced in this study was desirably smooth and flexible. This flexibility, in addition to hydrophobicity provides easy handling during implantation and a comfortable texture for use. Our FT-IR analysis revealed that the hydrophobic nature of these composite nanofibers in which the –OH related peak was significantly reduced compared to that of the pristine PU nanofibers.

XRD analysis was further used to investigate the phase structures of the PU, PU/Drug and PU/Drug/HA composite nanofibers. The XRD diffractograms of the composite nanofibers are shown in Fig. 2. The XRD patterns revealed that the PU/Drug/HA composite nanofibers were partially crystalline, whereas pristine PU nanofibers, and PU/Drug composite nanofibers were amorphous in nature. At the same time, the diffraction pattern corresponding to the PU/Drug composite nanofibers appears to be slightly sharper than that of the pristine nanofibers suggesting the presence of drug in the composite nanofiber structure. The presence of HA particles in the PU/Drug/HA composite nanofibers was confirmed by XRD which showed the diffraction peaks corresponding to the two clear peaks at 26.2° and 32.5° corresponding to (002) and (211) main reflection planes of apatite-like calcium phosphate (JCPDS no. 09-0432). However, in the case of PU/Drug composite nanofibers, the incorporation of drug did not reveal any structural changes due to low concentration. No significant diffraction peaks of any other phases or impurities can be detected in the XRD patterns, which indicate the successful formation of PU/Drug and PU/Drug/HA composite nanofibers.

The structural configurations of PU, PU/Drug and PU/Drug/HA composite nanofibers were characterized by using FT-IR spectroscopy. Fig. 3 illustrates the FT-IR spectra of the interaction between the PU nanofibers containing Drug and Drug/HA. The characteristic peaks of neat PU nanofibers can be assigned as 2950 cm^{-1} (CH_2 asymmetric vibration); 1750 cm^{-1} (free C–O); 1650 cm^{-1} (C═O bond); 1530 cm^{-1} (urethane amide II); 1081 cm^{-1} (C(O)–O–C stretching of the hard segment); and 821 cm^{-1} (bending vibration in benzene ring) [32,33]. The absorption band at 1375 cm^{-1} was due to the protonation of the amine group of the piperazine moiety. Some shifts were found in the FT-IR spectra of Drug blended PU composite nanofibers. The shift of the band of the protonated amine

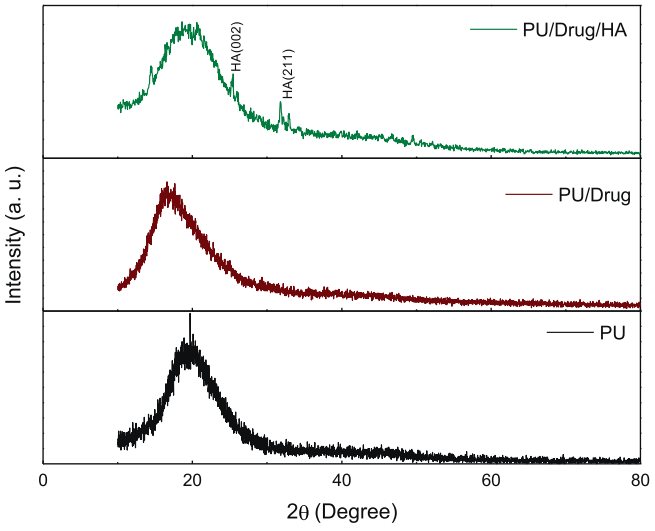

Fig. 2. XRD patterns of (a) PU, (b) PU/Drug, and (c) PU/Drug/HA composite nanofibers.

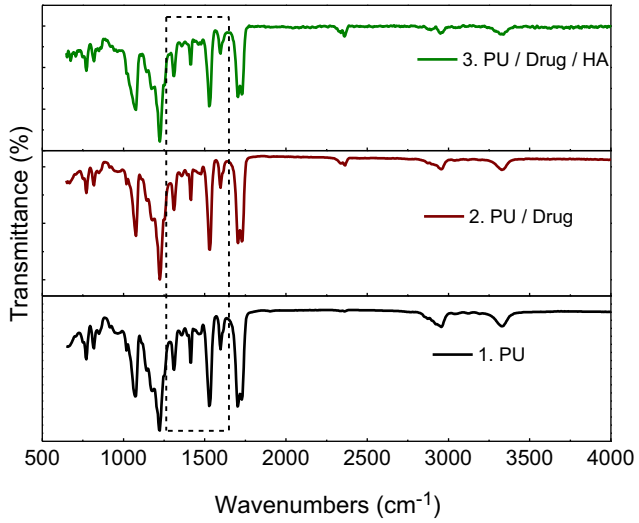

Fig. 3. FT-IR spectra of (a) PU, (b) PU/Drug, and (c) PU/Drug/HA composite nanofibers.

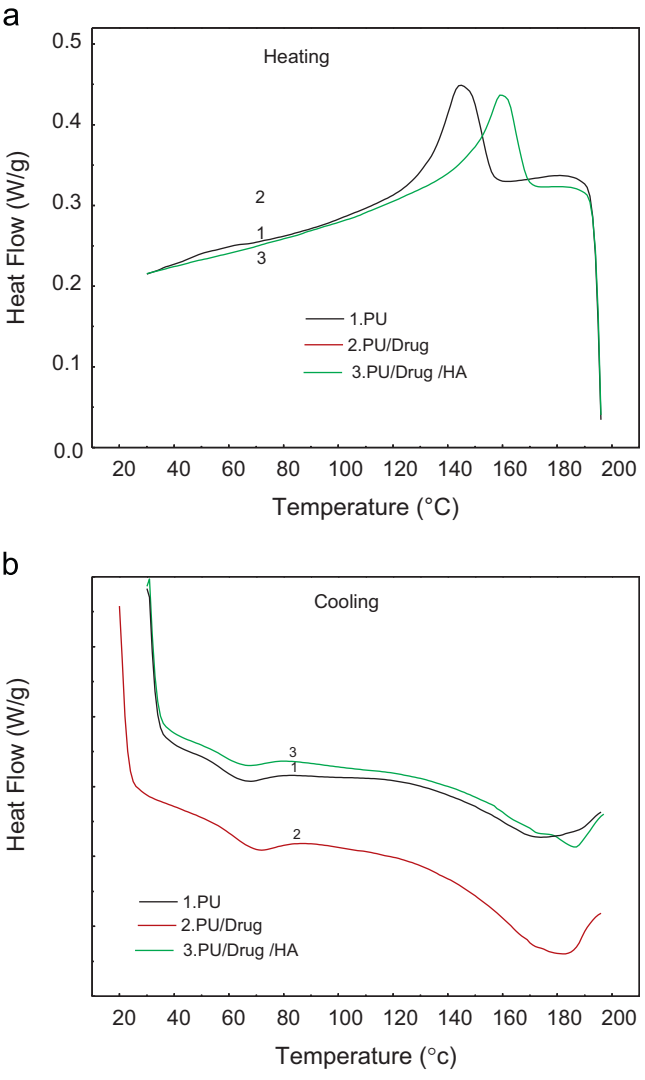

Fig. 4. DSC thermograms of pristine PU, PU/Drug and PU/Drug/HA composite nanofibers (a) heating and (b) cooling cylces.

group to 1393 cm^{-1} is suggesting the presence of electrostatic attraction between the protonated amine group and the polymer. It was observed that a broad transmittance band centered at 3500 cm^{-1} corresponding to –OH stretching vibration. One extra transmittance peak was observed for the PU/Drug/HA nanofibers at around 2225 cm^{-1} which is corresponding to CO_3^{2-} ions present in the sample. Comparing pristine PU with composite nanofibers, the peaks intensities were observed to be decreased with Drug and Drug/HA content. The significant change in the FT-IR spectra of these composite nanofibers is indicated as dotted box in Fig. 3. This may be due to the formation of hydrogen bonds among the components and the inter hydrogen bonds formed between two different macromolecules were stronger than those formed between the molecules of the same polymer. These FT-IR spectra result confirm the successful fabrication of drug incorporated PU composite nanofibers.

The changes in crystallinity of PU nanofibers containing Drug and Drug/HA nanoparticles upon thermal treatment were investigated by DSC at a heating rate of 10 °C/min, and the results are shown in Fig. 4. The pristine PU film showed a single melting peak at around 140 °C at the heating cycles as shown in Fig. 4(a). On the other hand, the melting peak was shifted to 160 and 170 °C for the PU composite nanofibers with Drug and Drug/HA, respectively which demonstrate the improved thermal properties of the composite nanofibers. The crystallinities of the PU composite nanofibers containing Drug and Drug/HA were improved as shown in Fig. 4(b). However, the pristine PU film did not show any significant crystallinity peak because of its amorphous nature.

Fig. 5 shows the TGA analyses of PU, PU/Drug and PU/HA/Drug composite nanofibers. The TGA results showed that all the samples were decomposed in a single step. The onset of decomposition of pristine PU, PU/Drug and PU/HA/Drug composite nanofibers were found to be in the range of 290–310 °C as shown in Fig. 5(a). This may be occurred due to the crystallinity of the drug and HA molecules. As expected the residual weight slightly increases with the addition of Drug and Drug/HA composites in the PU nanofibers. The data obtained in this study demonstrated a significant difference in the thermal

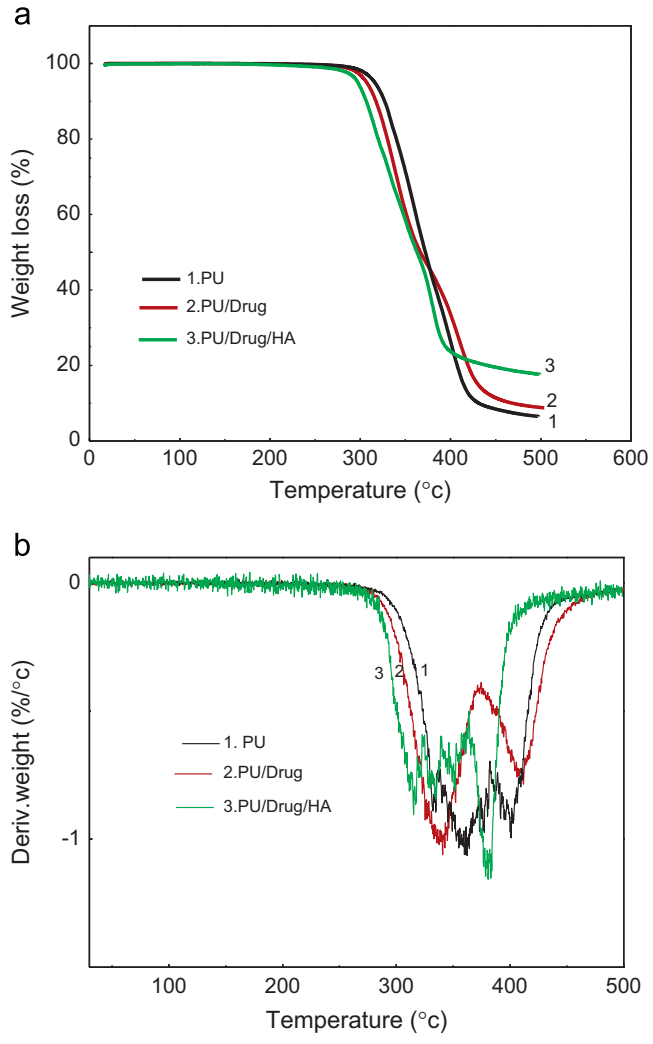

Fig. 5. (a) TGA traces pristine of pristine PU, PU/Drug and PU/Drug/HA composite nanofibers and (b) first derivative of TGA traces.

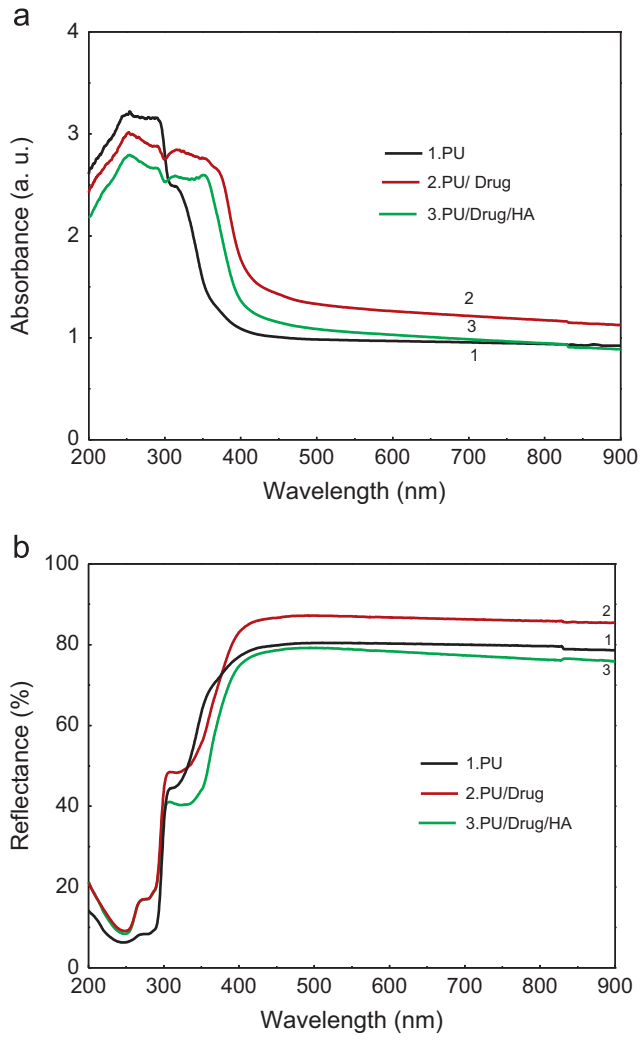

Fig. 6. UV–vis spectra of (a) PU, (b) PU/Drug, and (c) PU/Drug/HA composite nanofibers (a) absorbance, and (b) reflectance.

stabilities between the PU/Drug and PU/Drug/HA in comparison to electrospun pristine PU nanofibers. As shown in the first derivative data in Fig. 5(b), a single sharp peak appeared at 360 °C corresponding to pristine PU nanofibers, whereas two different peaks were observed at around 340 and 390 °C, respectively, for the PU/Drug and PU/Drug/HA composite nanofibers. These data are in good agreement with the DSC analysis.

Fig. 6 shows the UV–vis spectra of PU, PU/Drug and PU/Drug/HA composite nanofibers. As shown from the absorbance spectra in Fig. 6(a), the significant increase in the absorption at a wavelength lower than 300 nm can be observed corresponding to the PU nanofibers containing PU/Drug and PU/Drug/HA nanoparticles. The absorbance intensity was increased with the addition of PU/Drug and PU/Drug/HA in PU nanofibers, which was attributed to the significant enhancement of light absorption in the visible light region. These observations showed that the absorption edge of PU can be engineered toward longer wave length by the introduction of HA and Drug in the PU nanofibers. The respective reflectance spectra of these composite nanofibers are shown in Fig. 6(b). As expected, the reflectance intensity was reduced with the addition of HA and Drug in the PU nanofibers. It was illustrated that the incorporation of HA and in PU nanofibers could effectively block the UV region (200–300 nm). The reflectance was decreased with the addition of HA and Drug in the PU nanofibers which can be attributed the effective absorbance of UV emissions by

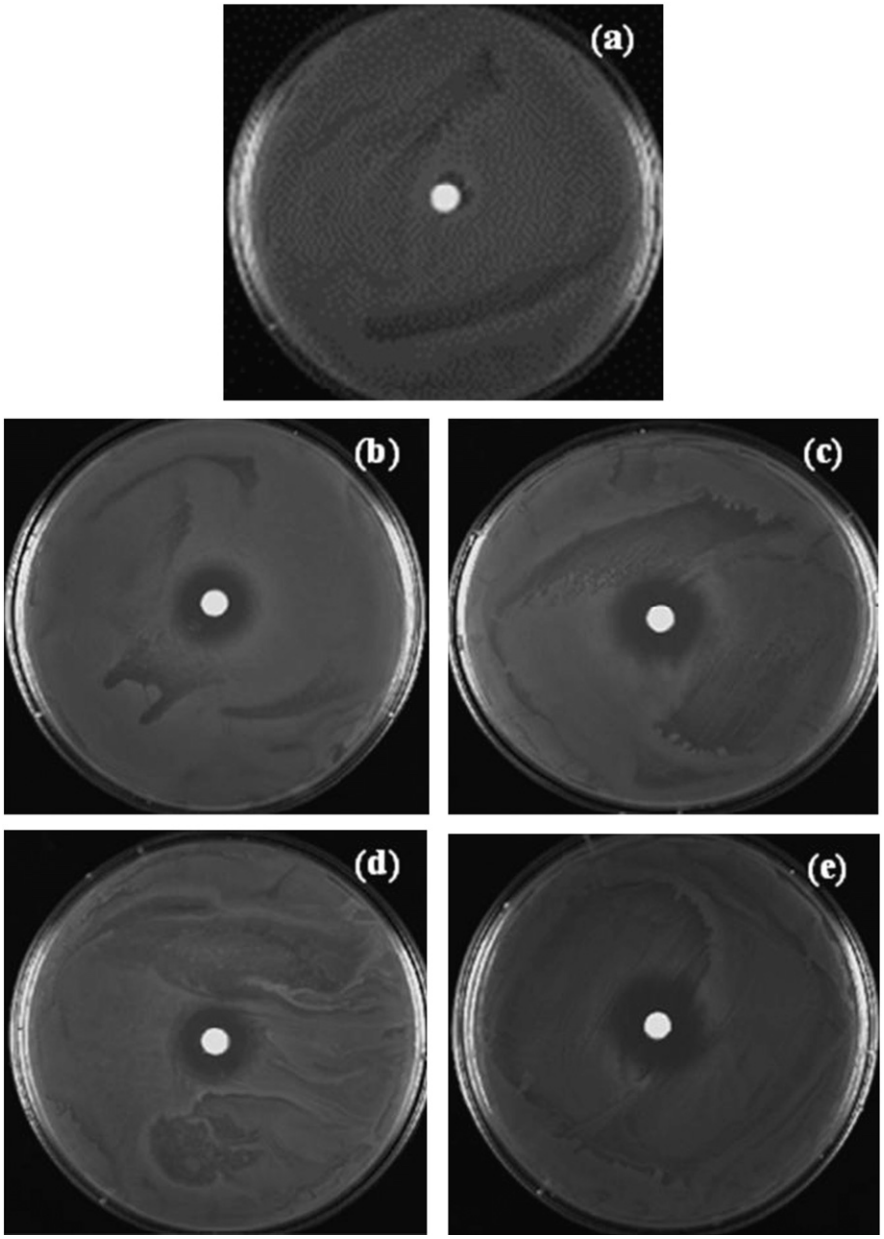

Fig. 7. Bactericidal activity of *Staphylococcus aureus* and *Escherichia coli*, exposed to pristine PU (a), PU/Drug (b,d), and PU/Drug/HA (c,e) composite nanofibers.

the particles counterpart homogeneously present in the thin film. Such kind of characteristics of these thin films are of more important as per technological applications like antibacterial activity is concerned.

The effect of bactericidal activity of PU/Drug and PU/Drug/HA composite nanofibers in the culture media was studied by the disc diffusion susceptibility test, with MHA medium containing *S. aureus*, *E. coli*, bacterial strains separately, after 24 h of incubation. No bactericidal activity was detected for the pristine PU as shown in Fig. 7(a), which was the actual diameter of the PU nanofibers disc (6 mm). However, more pronounced bactericidal effect was observed for the PU/Drug and PU/Drug/HA composite nanofibers, as shown in Fig. 7(b)–(e). The test was repeated and the results were found to be almost same. The plates were checked for the prolonged incubation time to check the efficiency of the drug release. As observed from the disc diffusion test, the efficacy of the PU/Drug and PU/Drug/HA is similar that of PU nanofibers. It has been a known factor that the decontamination of exogenous organisms is a critical factor for a wound healing material; the antibacterial property plays a crucial role for the electrospun-based wound dressing membranes. As the interconnected nanofibers create a perfect blocks and pores in nanofiber membrane, the nanofiber membrane should be able to prevent any bacteria from penetrating, therefore avoiding the exogenous infections effectively. The results showed that our composite mat is a good antibacterial membrane and it can be applied as a perfect wound dressing material.

In our results, when compare with the PU/Drug and PU/Drug/HA composite nanofibers, PU/Drug/HA composite nanofibers showed that strong bactericidal activity for both Gram-positive *S. aureus,* and Gram-negative *E. coli*. This is because there were plenty of drug particles can be readily available on the periphery of the nanofibers sample. Thus, we can conclude that the obtained PU/Drug/HA and PU/Drug composite nanofibers are predicted as a desirable candidate to be utilized for excellent antimicrobial filters and also wound healing agents.

4. Conclusions

In summary, we have successfully obtained Drug and HA/Drug blended PU composite nanofibers via the electrospinning technique. The XRD data clearly confirmed the presence of apatite-like materials in the PU nanofibers containing Drug/HA nanoparticles. The FT-IR analysis of the PU, PU/Drug and PU/Drug/HA composite nanofibers indicate that the PO_4^{3-} and CO_3^{2-} content in the sample, confirmed the presence of calcium phosphates. However, the question of potential cytotoxicity of drug present in the composite nanofibers needs to be further addressed. The drug incorporated PU composite nanofibers exhibited excellent antibacterial property toward *S. aureus*, *E. coli* bacterial strains. PU/Drug/HA composite nanofibers were able to significantly reduce the number of pathogenic cells adherent per polymer unit surface with respect to the pristine PU. Overall, the PU/Drug/HA and PU/Drug composite nanofibers are very promising materials for the multipurpose applications such as, antibacterial packaging, filtration, and wound dressing and so on. Results of these studies will likely to open the new directions for the future investigation of Drug/HA nanoparticles-containing polymers based materials for the various other applications.

Acknowledgments

This research was financially supported by the Ministry of Education, Science Technology (MEST) and the National Research Foundation of Korea (NRF) through the Human Resource Training Project for Regional Innovation. One of the authors R. Nirmala kindly acknowledges the research funds supported by the Chonbuk National University for the year 2012–2015.

References

[1] H. Daemi, M. Barikani, M. Barmar, Compatible compositions based on aqueous polyurethane dispersions and sodium alginate, Carbohydrate Polymers 92 (2013) 490–496.
[2] A.M. Castagna, D. Fragiadakis, H. Lee, C. Choi, J. Runt, The role of hard segment content on the molecular dynamics of poly(tetramethylene oxide)-based polyurethane copolymers, Macromolecules 44 (2011) 7831–7836.
[3] Q.B. Meng, S.I. Lee, C. Nah, Y.S. Lee, Preparation of waterborne polyurethanes using an amphiphilic diol for breathable waterproof textile coatings, Progress in Organic Coatings 66 (2009) 382–386.
[4] J.R. Basford, M.A. Smith, Shoe insoles in the workplace, Orthopedics 11 (1988) 285–288.
[5] H.M.C. De Azeredo, Nanocomposites for food packaging applications, Food Research Internation 42 (2009) 1240–1253.
[6] D.R. Paul, L.M. Robeson, Polymer nanotechnology: nanocomposites, Polymer 49 (2008) 3187–3204.
[7] P.R. Chang, R. Jian, P. Zheng, J. Yu, X. Ma, Preparation and properties of glycerol plasticized-starch (GPS)/cellulose nanoparticle (CN) composites, Carbohydrate Polymer 79 (2010) 301–305.
[8] I.Y. Jeon, J.B. Baek, Nanocomposites derived from polymers and inorganic nanoparticles, Materials 3 (2010) 3654–3674.
[9] D. Kim, K. Jeon, Y. Lee, J. Seo, K. Seo, H. Han, S.B. Khan, Preparation and characterization of UV-cured polyurethane acrylate/ZnO nanocomposite films based on surface modified ZnO, Progress in Organic Coatings 74 (2012) 435–442.
[10] P. Supaphol, O. Suwantong, P. Sansanoh, S. Sowmya, R. Jayakumar, S.V. Nair, Electrospinning of biocompatible polymers and their potentials in biomedical applications, Advances in Polymer Science 246 (2012) 213–240.
[11] P. Sikareepaisan, U. Ruktanonchai, P. Supaphol, Preparation and characterization of asiaticoside-loaded alginate films and their potential for use as effectual wound dressings, Carbohydrate Polymers 83 (2011) 1457–1469.
[12] B.L. Davis, D.A. Dixon, E.B. Garner, J.C. Gordon, M.H. Matus, B.L. Scott, Efficient regeneration of partially spent ammonia borane fuel, Angewandte Chemie International 48 (2009) 6812–6816.
[13] D.H. Reneker, I. Chun, Nanometre diameter fibres of polymer produced by electrospinning, Nanotechnology 7 (1996) 216–223.
[14] T.L. Tsou, S.T. Tang, Y.C. Huang, J.R. Wu, J.J. Young, H.J. Wang, Poly (2-hydroxyethyl methacrylate) wound dressing containing ciprofloxacin and its drug release studies, Journal of Materials Science: Materials in Medicine 16 (2005) 95–100.
[15] K. Dillen, J. Vandervoort, G. Van den Mooter, L. Verheyden, A. Ludwig, Factorial design, physicochemical characterization and

activity of ciprofloxacin–PLGA nanoparticles, International Journal of Pharmaceutics 275 (2004) 171–187.
[16] D.W. Hutmacher, J.T. Schantz, C.X.T. Lam, K.C. Tan, T.C. Lim, State of the art and future directions of scaffold based bone engineering from a biomaterials perspective, Journal of Tissue Engineering Regeneration Medicine 1 (2007) 245–260.
[17] W. Habraken, J.G.C. Wolke, J.A. Jansen, Ceramic composites as matrices and scaffolds for drug delivery in tissue engineering, Advanced Drug Delivery Review 59 (2007) 234–248.
[18] M.P. Ginebra, T. Traykova, J.A. Planell, Calcium phosphate cements as bone drug delivery systems: a review, Journal of Control Release 113 (2006) 102–110.
[19] M.P. Ginebra, T. Traykova, J.A. Planell, Calcium phosphate cements: competitive drug carriers for the musculoskeletal system?, Biomaterials 27 (2006) 2171–2177
[20] H. Zhou, J. Lee, Nanoscale hydroxyapatite particles for bone tissue engineering, Acta Biomaterialia 7 (2011) 2769–2781.
[21] W.J. Shih, Y.F. Chen, M.C. Wang, M.H. Hon, Crystal growth and morphology of the nano-sized hydroxyapatite powders synthesized from $CaHPO_4$–$2H_2O$ and $CaCO_3$ by hydrolysis method, Journal of Crystal Growth 270 (2004) 211–218.
[22] T.A. Kuriakose, S.N. Kalkura, M. Palanichamy, D. Arivuoli, K. Dierks, G. Bocelli, Synthesis of stoichiometric nano crystalline hydroxyapatite by ethanol-based sol–gel technique at low temperature, Journal of Crystal Growth 263 (2004) 517–523.
[23] S. Sarig, F. Kahana, Rapid formation of nanocrystalline apatite, Journal of Crystal Growth 237 (2002) 55–59.
[24] S. Bose, S.K. Saha, Synthesis of hydroxyapatite nanopowders via sucrose templated sol–gel method, Journal of American Ceramic Society 86 (2003) 1055–1057.
[25] N. Kivrak, A. Ta, Synthesis of calcium hydroxyapatite tricalcium phosphate (HA TCP) composite bioceramic powders and their sintering behavior, Journal of the American Ceramic Society 81 (1998) 2245–2252.
[26] R.A. Young, D.W. Holcomb, Variability of hydroxyapatite preparations, Calcified Tissue International 34 (1982) S17–S21.
[27] L. Bernard, M. Freche, J.L. Lacout, B. Biscans, Preparation of hydroxyapatite by neutralization at low temperature-influence of purity of the raw material, Powder Technology 103 (1999) 19–25.
[28] H.S. Liu, T.S. Chin, L.S. Lai, S.Y. Chiu, K.H. Chung, C.S. Chang, Hydroxyapatite synthesized by a simplified hydrothermal method, Ceramics International 23 (1997) 19–25.
[29] G.K. Lim, J. Wang, S.C. Ng, C.H. Chew, L.M. Gan, Processing of hydroxyapatite via microemulsion and emulsion routes, Biomaterials 18 (1997) 1433–1439.
[30] W.L. Suchanek, P. Shuk, K. Byrappa, R.E. Riman, K.S. TenHuisen, V.F. Janas, Mechanochemical-hydrothermal synthesis of carbonated apatite powders at room temperature, Biomaterials 23 (2002) 699–710.
[31] R. Nirmala, R. Navamathavan, R. Afeesh, H.-M. Park, H.-S. Kang, H.Y. Kim, Characterisation of bioresourced hydroxyapatite containing silver nanoparticles, Materials Research Innovations 16 (2012) 249–256.
[32] S.S.L. Sobhana, J. Sundaraseelan, S. Sekar, T.P. Sastry, A.B. Mandal, Gelatin–chitosan composite capped gold nanoparticles: a matrix for the growth of hydroxyapatite, Journal of Nanoparticles Research 11 (2009) 333–339.
[33] T.P. Sastry, J. Sundaraseelan, K. Swarnalatha, S.S.L. Sobhana, M.U. Makheswari, S. Sekar, A.B. Mandal, Growth of hydroxyapatite on physiologically clotted fibrin capped gold nanoparticles, Nanotechnology 19 (2008) 245604.